Journal of Physics and Its Applications

Journal homepage : https://ejournal2.undip.ac.id/index.php/jpa/index

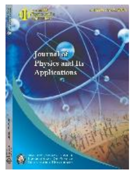

Generation of monocycle efficient terahertz pulses by optical rectification in $LiNBO_3$ at 800 nm

Ali Khumaeni,[1,2*] Hideaki Kitahara,[1] Takashi Furuya,[1] Kohji Yamamoto,[1] and Masahiko Tani[1]

[1]*Research Center for Development of Far Infrared Region, University of Fukui, Bunkyo 3-9-1, Fukui 910-8507, Japan*
[2]*Department of Physics, Faculty of Science and Mathematics, Diponegoro University, Jl. Prof. Soedharto, S.H., Tembalang, Semarang 50275, Indonesia*

ARTICLE INFO

Article history:
Received : September 2018
Accepted : November 2018
Available online : November 2018

Keywords:
Efficient terahertz pulse generation
Optical rectification
Tilted pump pulse front scheme
Femtosecond laser
$LiNbO_3$ crystal

ABSTRACT

Generation of efficient terahertz (THz) pulses was experimentally made by tilted pump pulse front scheme with a Mg-doped $LiNbO_3$ crystal. In this study, a spitfire laser (Ti:sapphire laser, 800 nm, 3 mJ, 1 kHz) was used as an optical source for the generation and detection of THz pulses. The electro-optic (EO) detection optics consisting of a ZnTe crystal (1 mm in thickness) and a balanced photodetector was used. To obtain optimum THz characteristics and pump to THz power conversion efficiency, the image of the grating was made coincides with the tilted pump pulse front. The maximum THz electric field of 8.5 kV/cm and the frequency bandwidth of 2.5 THz were achieved by using pump pulse energy of 2.4 mJ and pump pulse width of 100 fs. The THz energy of 4.15 μJ was obtained and pump-to-THz conversion efficiency was estimated to be approximately 1.73 x 10^{-3}.

1. Introduction

Terahertz band in the frequency rage of at 0.1-10 THz has attracted many scientists due to its potential for fundamental science and various applications [1, 2]. In this area, the research activities are directed to the applications of THz pulses in time-domain THz spectroscopy and THz imaging [3-5]. Advanced applications of THz radiation pulses are detection of intermolecular vibrations [6,7], understanding of carrier dynamics in semiconductors [8], nondestructive testing [9], and new approach of medical diagnostic and treatment [10,11]. Specifically, THz radiation pulses are also employed to study nonlinear transport phenomena in various solid materials [12]. To this point, high-intense THz pulses with an energy of several μJ are required.

Various works have been carried out for the generation of intense THz pulse. Knippels et al. generated THz pulses using free electron laser sources [13]. The THz pulse energy was achieved at least 1 μJ. The other common method for intense THz generation is photoconductive (PC) antennas based on semiconductor materials, which is usually used for terahertz time domain spectroscopy (THz-TDS) [14-16]. However, it is not scalable to large pulse energies due to saturation of the THz electric field amplitude.

To generate high intense THz pulses, Hebling et al. proposed a tilted pump pulse front scheme for efficient phase matched THz pulse from nonlinear crystal $LiNbO_3$ (LN) [17-19]. Tilting the pump pulse front allows one to match the optical group velocity and the THz velocity, resulting in a far higher conversion efficiency. In the original experiment, tilting of the pulse front was realized by diffracting the pump beam off a diffraction grating and subsequently imaging it onto the LN crystal [20]. The technique has demonstrated the possibility of THz-pulse generation with energies on the scale of 10 μJ by using Ti:sapphire laser with low repetition frequencies [21]. To generate a high-intense THz pulses, various related parameters should be considered. Careful arrangement of experimental setup is urgently necessary. However recent analysis of the experimental arrangement certified that the imaging errors by grating and lenses in the setup can cause the distortion in the generated THz intensity [22]. Hirori et al. has generated intense THz pulses using 4f-lens arrangement utilizing tilted pump pulse front (TPPF) scheme with $LiNbO_3$. The THz detection system included GaP crystal.

In this paper, the generation of high-intense single-cycle THz pulses was carried out by utilizing TPPF with Mg-doped $LiNbO_3$ crystal and ZnTe crystal as a part of detection system. To obtain optimal THz beam characteristics and pump to THz conversion efficiency, the image of the grating was coincided with the tilted pulse front.

1. Experimental procedure

The experimental setup of the THz pulse generation using TPPF scheme and the electro-optic (EO) sampling was shown in Fig. 1. A femtosecond laser (Spitfire, intensified Ti:sapphire laser, 800 nm, 100 fs, 1 kHz) was used as an optical source for the generation and detection of THz emission. The laser pulses were split into pump and probe beams by an optical sapphire window (Sigma Koki). The pump beam was sent to the grating (groove density of 1800 mm^{-1}) with an angle of incident of 37^0. The pump beam diffracted from the grating was imaged onto the $LiNbO_3$ crystal using two cylindrical lenses L_1 and L_2 with a focal length of 150 mm and 100 mm, respectively. A half wave plate between L_1 and L_2 was used to change the direction of polarization from horizontally to vertically direction.

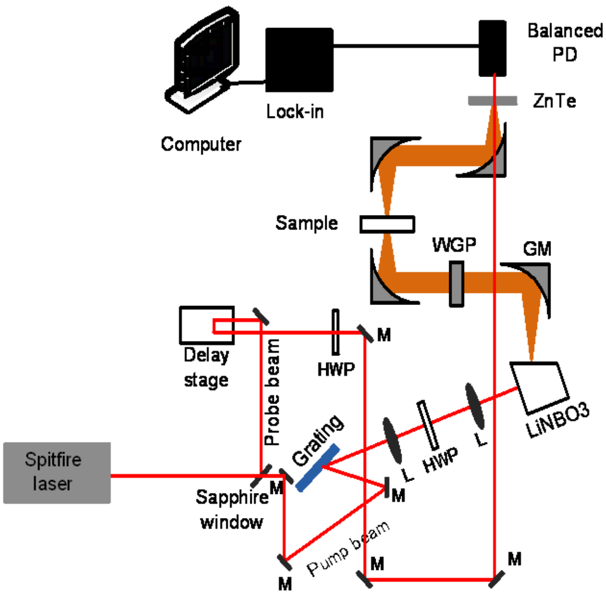

Fig. 1: Experimental setup used in this work.

THz radiation was generated from the crystal and guided with four off-axis parabolic gold mirrors of different focal lengths to the electro-optic (EO) detection optics consisting of ZnTe crystal (t = 1 mm) and a balanced photodetector (ABL-100, Zomega Corp.). In the balanced detector, the probe beam was $\pi/2$ phase biased with a quarter waveplate and divided into the vertical and horizontal polarization components (IA and IB) with a Wollaston prism. Each component was detected by a pair of photodiodes (A and B). The different signal from the two photodiodes was fed to the lock in amplifier. The EO signal is given as $\triangle I/I$ = (IA-IB)/(IA+IB) = $\triangle V$/VA+VB). The time-domain THz waveform was obtained in a standard terahertz time domain spectroscopy (THz-TDS) scheme. The sample was placed at the focal point of THz beam in the four parabolic mirror system. All the measurements were conducted at room temperature at around 20^{0}C.

2. Results and discussion

First, the effect of the incident laser pump power to the generated THz electric field was examined. The energy of pump pulse was varied from 0.1 to 2 mJ.
The measurement was carried at 1 kHz repetition rate and 100 fs laser pulse width. Figure 2 shows how THz electric field amplitude changes with the incident pump pulse energy. The THz electric field quadratically increased with increasing of pump power.

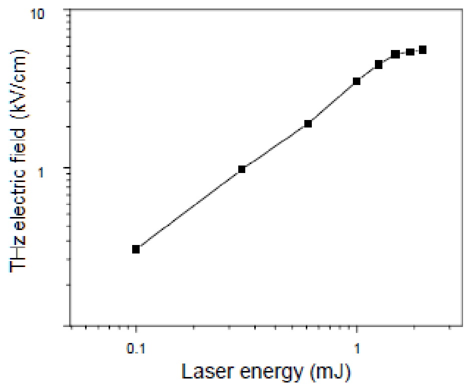

Fig. 2: Effect of laser energy to THz electric field.

However, it should be noted that at high laser pump energy of above 1.5 mJ, the amplitude of THz electric field was saturated, which might be due to the free carrier absorption of THz pulses in $LiNbO_3$ crystal as reported in the previous paper [23]. This result confirmed the previous experimental works [22, 24] that a quadratic dependence of pump pulse energy clearly occurs at low pumping level.

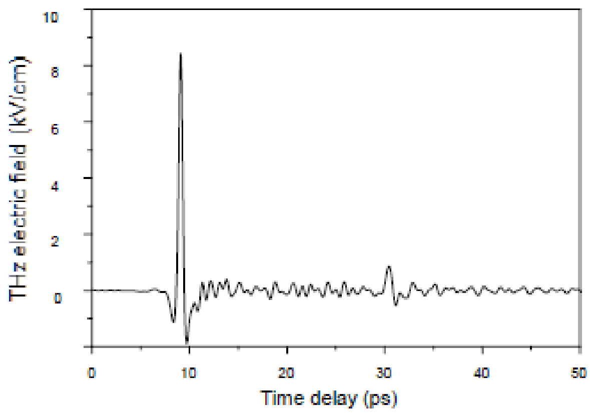

(a)

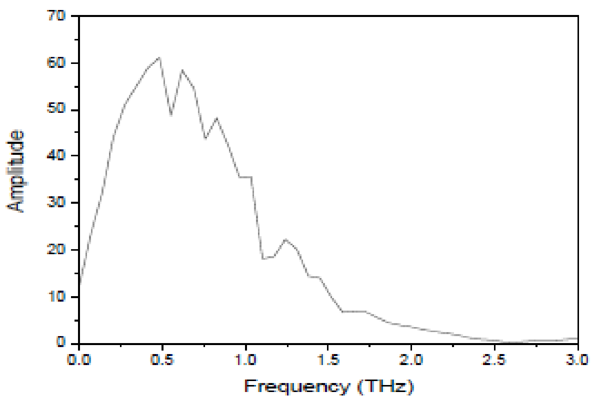

(b)

Fig. 3: (a) Temporal profile measured by THz electro-optic sampling, (b) THz spectrum obtained by fast Fourier transform.

Shown in Fig. 3(a) and 3(b) are THz temporal profile measured by THz electro-optic (EO) sampling with a 1 mm thick ZnTe crystal and the corresponding THz spectrum obtained by fast Fourier transform, respectively. To determine the strength of THz electric field, this following formula was employed, [25]

$$\frac{\Delta V}{V} = \frac{2\pi}{\lambda} n_0^3 r_{41} E_{THz} d \qquad (1)$$

where E_{THz} is THz electric field (V/cm), λ is the wavelength of the laser pump beam(nm), r_{41} is the electro-optic coefficient with 4.04 pm/V for ZnTe. d and n_0 are thickness of the ZnTe crystal (1 mm) and refractive index of the optical crystal with 2.85 for ZnTe. △V and V are voltage of lock in output induced by THz signal and sum of absolute voltage photodetector A (PD-A) and photodetector B (PD-B) in balanced detector, respectively. By using the present setup (Fig. 1) and Eq. 1, the strength of THz electric field with amplitude of approximately 8.5 kV/cm was achieved by laser pump pulse with a laser energy of 2.4 mJ and a laser pulse width of 100 fs.

Figure 3(b) shows the Fourier component of the THz emission measured by THz EO sampling with a ZnTe detection crystal (thickness of 1 mm). The frequency spectrum containing THz spectral components spans up to approximately 2.5 THz. The center frequency and the full width at half maximum (FWHM) of the THz spectrum were 0.72 THz and 1.00 THz, respectively.

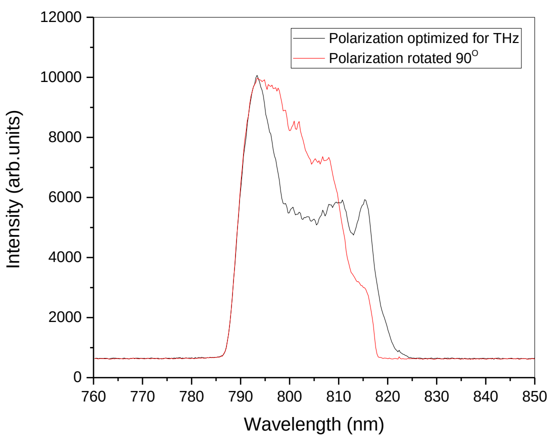

Fig. 4: Spectrum of the pump beam after the LN crystal.

The THz conversion efficiency was estimated by redshift, which is experimentally measured. Figure 4 shows the spectrum of the pump beam after the LN crystal, which was measured by using an Ocean Optics (HR4000CG-UV-NIR). The laser energy was fixed at 2.4 mJ and the laser pulse width was 100 fs. After passing through a LN crystal, laser pump beam spectrum shows a redshift at optimum THz output. This effect happens only when the pump beam was polarized for THz generation. The redshift takes place due to the difference frequency generation (DFG) process in the LN crystal. The total shift △λ in the spectrum was calculated using following formula [24],

$$\bar{\lambda} = \frac{\int \lambda S(\lambda) d\lambda}{\int S(\lambda) d\lambda} \qquad (1)$$

Average wavelength value of 802.2 nm and 800.8 nm were obtained for the redshift spectrum (black line in Fig. 5) and the spectrum with crossed polarization (no THz generation), yielding a spectrum averaged redshift $(\bar{\lambda})$ of 1.38 nm in the case of optimum efficient THz generation. First spectral moment of the frequency spectrum from Fig. 3(b) as in Eq.1 was obtained with a value of 0.72 THz. Wavelength shift in the optical spectrum is calculated as follows [24],

$$\Delta\lambda_{exp} = \frac{c}{v^2} \Delta v \qquad (2)$$

Using Eq. 2, the wavelength shift was 1.54 nm. By comparing the observed optical redshift to the wavelength shift, a photon efficiency of 90% was obtained. Using this result, energy of generated THz pulses can be estimated using this following formula [25],

$$E_{THz\ pulse} = h v_{THz} \cdot \frac{E_{pump}}{h v_{pump}} \qquad (3)$$

The THz energy of 4.15 μJ was obtained using Eq. 3.

Conclusions

High-intense THz pulses has been generated by using a tilted pulsed front scheme with a Mg-doped $LiNbO_3$ crystal. Optimum THz electric field of approximately 8.5 kV/cm was achieved by a laser pump energy of 2.4 W. Careful arrangement of tilted pump pulse front improved the characteristics of THz pulses with an optimum pump to THz conversion efficiency. The THz energy of 4.15 μJ was obtained and pump-to-THz conversion efficiency was estimated to be approximately 1.73 x 10^{-3}.

References

1. M. Tonouchi, “Cutting-edge terahertz technology”, Nat. Photonics **1**, 97-105 (2007).
2. D. Saeedkia, Handbook of Terahertz Technology for Imaging, Sensing, and Communications (Woodhead Publishing, Oxford, 2013).
3. J. Orenstein and J. S. Dodge, “Terahertz time-domain spectroscopy of transient metallic and superconducting states”, Phys. Rev. B **92**, 134507 (2015).
4. E. Castro-Camus, M. Palomar, and A. A. Covarrubias, “Leaf water dynamics of Arabidopsis thaliana monitored in-vivo using terahertz time-domain spectroscopy”, Scientific Reports **3**, 2910 1-5(2013).
5. K. I. Zaytsev, A. A. Gavdush, S. P. Lebedev, V. E. Karasik, S. O. Yurchenko, “A method of studying spectral optical characteristics of a homogeneous medium by means of terahertz time-domain spectroscopy”, Optics and Spectroscopy **118**, 552-562 (2015).
6. R. Li, J. A. Zeitler, D. Tomerini, E. P. J. Parrot, L. F. Gladden, and G. M. Day, “A study into the effect of subtle structural details and disorder on the terahertz spectrum of crystalline benzoic acid”, Phys. Chem. Chem. Phys. **12**, 5329-5340 (2010).

7. A. I. McIntosh, B. Yang, S. M. Goldup, M. Watkinson, and R. S. Donnan, "Terahertz spectroscopy: a powerful new tool for the chemical sciences?", Chem. Soc. Rev. **41**, 2072-2082 (2012).
8. R. Ulbricht, E. Hendry, J. Shan, T. F. Heinz, and M. Bonn, "Carrier dynamics in semiconductors studied with time-resolved terahertz spectroscopy", Rev. Mod. Phys. **83**, 543 (2011).
9. K. H. Jin, Y. –G. Kim, S. H. Cho, J. C. Ye, D. –S. Ye, High-speed terahertz reflection three-dimensional imaging for nondestructive evaluation", Opt. Express **20**, 25432-25440 (2012).
10. T. Ouchi, K. Kajiki, T. Koizumi, T. Itsuji, Y. Koyama, R. Sekiguchi, O. Kubota, and K. Kawase, Terahertz imaging system for medical applications and related high efficiency terahertz devices", J. Infrared, Millimeter, and Terahertz Waves **35**, 118-130 (2014).
11. E. P. J. Parrot, Y. Sun, E. P. –MacPherson, Terahertz spectroscopy: its future role in medical diagnoses", J. Molec. Struct. **1006**, 66-76 (2011).
12. H. Hirori and K. Tanaka, "Nonlinear optical phenomena induced by intense single-cycle terahertz pulses", IEEE J. Selected Topic in Quantum Electronics **19**, 8401110 (2013).
13. G. M. H. Knippels, R. F. X. A. M. Mols, A. F. G. Van der Meer, D. Oepts, P. W. van Amersfoort, "Intense far-infrared free-electron laser pulses with a length of six optical cycles", Phys. Rev. Lett. **75**, 1755 (1995).
14. S. L. Dexheimer, Terahertz Spectroscopy: Principles and Applications (CRC Press, Taylor and Francis Group, Boca Raton, 2008).
15. M. Beck, H. Schäfer, G. Klatt, J. Demsar, S. Winnerl, M. Helm, and T. Dekorsy, "Impulsive terahertz radiation with high electric fields from an amplifier-driven large-area photoconductive antenna", Opt. Express **18**, 9251-9257 (2010).
16. A. Dreyhaupt, S. Winnerl, T. Dekorsy, and M. Helm, "High-intense terahertz radiation from a microstructured large-area photoconductor", Appl. Phys. Lett. **86**, 121114 (2005).
17. J. Hebling, G. Almási, I. Z. Kozma, and J. Kuhl, "Velocity matching by pulse front tilting for large-area THz-pulse generation", Opt. Express **10**, 1161-1166 (2002).
18. J. Hebling, A. G. Stepanov, G. Almási, B. Bartal, and J. Kuhl, "Tunable THz pulse generation by optical rectification of ultrashort laser pulses with tilted pulse front", Appl. Phys. B **78**, 593-599 (2004).
19. J. Hebling, K. –L. Yeh, M. C. Hoffmann, B. Bartal, and K. A. Nelson, "Generation of high-power terahertz pulses by tilted-pulse-front excitation and their application possibilities", J. Opt. Soc. America B **25**, B6-B19 (2008).
20. K. –L. Yeh, J. Hebling, M. C. Hoffmann, and K. A. Nelson, "Generation of high average power 1 kHz shaped THz pulses via optical rectification", Opt. Communications **281**, 3567-3570 (2008).
21. K.-L. Yeh, M. C. Hoffmann, J. Hebling, and K. A. Nelson, "Generation of 10 μJ ultrashort terahertz pulses by optical rectification", Appl. Phys. Lett. **90**, 171121 (2007).
22. J. A. Fülöp, L. Pálfalvi, G. Almási, and J. Hebling, "Design of high-energy terahertz sources based on optical rectification", Opt. Express **18**, 12311-12327 (2010).
23. J. A. Fülöp, L. Pálfalvi, S. Klingebiel, G. Almási, F. Krausz, S. Karsch, and J. Hebling, "Generation of sub-mJ terahertz pulses by optical rectification", Opt. Lett. **37**, 557-559 (2012).
24. M. C. Hoffmann, K. –L. Yeh, J. Hebling, and K. A. Nelson, "Efficient terahertz generation by optical rectification at 1035 nm", Opt. Express **15**, 1170611713 (2007).
25. F. Blanchard, L. Razzari, H. C. Bandulet, G. Sharma, R. Morandotti, J. C. Kieffer, T. Ozaki, M. Reid, H. F. Tiedje, H. K. Haugen, and F. A. Hegmann, "Generation of 1.5 μJ single-cycle terahertz pulses by optical rectification from a large aperture ZnTe crystal", Opt. Express **15**, 13212-13220 (2007).